SLAC-PUB-10813
October 2004

Nuclear models in FLUKA: present capabilities, open problems and future improvements

F. Ballarini*, G. Battistoni†, F. Cerutti†, A. Empl**, A. Fassò‡, A. Ferrari§†, E. Gadioli†, M.V. Garzelli†, A. Ottolenghi*, L.S. Pinsky**, J. Ranft¶, S. Roesler§, P. R. Sala† and G. Smirnov‖

*University of Pavia and INFN, Italy
†University of Milan and INFN, Italy
**Houston University, Texas, USA
‡SLAC, Stanford, USA
§CERN
¶Siegen University, Germany
‖JINR, Dubna, Russia

Abstract. The nuclear reaction models embedded in the FLUKA code cover hadron, ion, photon and neutrino induced nuclear interactions from energies as low as few tens of MeV up to several tens of TeV. A short description of the main physics ingredients in the FLUKA nuclear models is given, with emphasis on the intermediate energy range and on "exotic" reactions. The treatment of electromagnetic dissociation as recently implemented in FLUKA is described. Examples of performances are presented for illustrative situations covering some of the most typical FLUKA applications.

INTRODUCTION

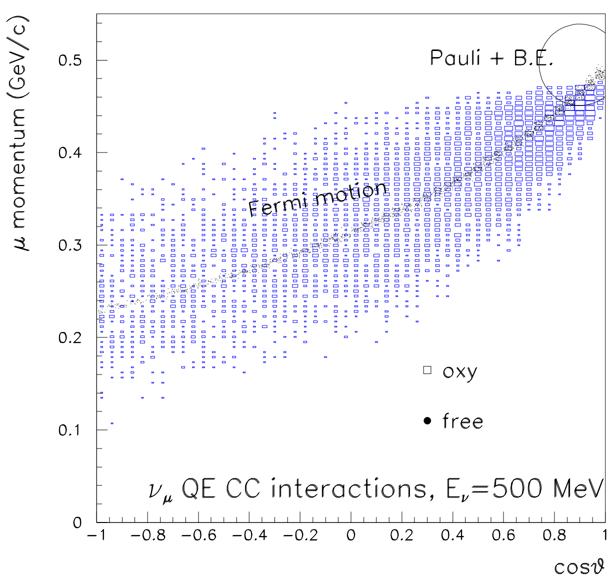

FIGURE 1. Momentum-angle correlation of μ from Quasi Elastic Charged Current interactions of ν_μ on free neutrons and on Oxygen nuclei

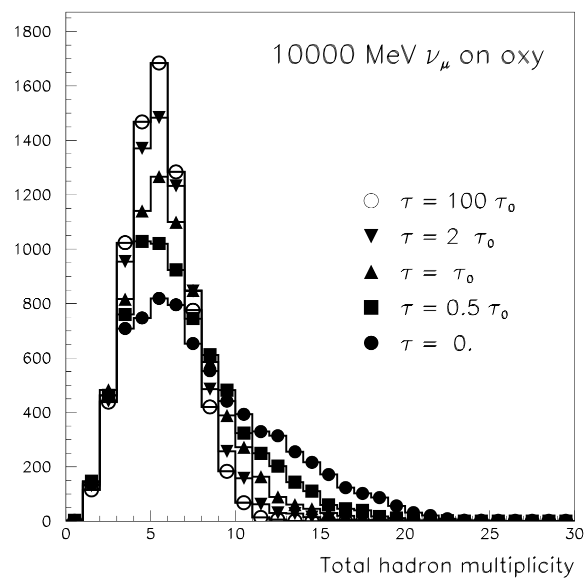

FIGURE 2. Effect of different formation time (τ) values on the charged hadron multiplicity in 10 GeV ν_μ CC interactions on Oxygen.

FLUKA [1] is a Monte Carlo code able to simulate interaction and transport of hadrons, heavy ions and electromagnetic particles from few keV (or thermal neutron) to cosmic ray energies in wichever material. It has

Work supported in part by the Department of Energy, contract DE-AC02-76SF00515

Stanford Linear Accelerator Center, Stanford University, Stanford, CA 94309

Presented at the International Conference on Nuclear Data for Science and Technology (ND2004), 9/26/2004 - 10/1/2004, Santa Fe, NM

proven capabilities in accelerator design and shielding, ADS studies and experiments, dosimetry and hadrotherapy, space radiation and cosmic ray shower studies in the atmosphere. The highest priority in the design and development of FLUKA has always been the implementation and improvement of sound and modern physical models. Microscopic models are adopted whenever possible, consistency among all the reaction steps and/or reaction types is ensured, conservation laws are enforced at each step, results are checked against experimental data at single interaction level. As a result, final predictions are obtained with a minimal set of free parameters fixed for all energy/target/projectile combinations. Therefore results in complex cases, as well as properties and scaling laws, arise naturally from the underlying physical models, predictivity is provided where no experimental data are directly available, and correlations within interactions and among shower components are preserved. Thanks to their accuracy and generality, the FLUKA hadronic models offer a suitable environment for "exotic" applications, like neutrino interactions and nucleon decay. Neutrino experiments are becoming more and more demanding on terms of simulation reliability and precision as they aim to study low probability processes like sub-leading oscillations or CP violation. Nuclear effects on neutrino interactions can have heavy consequences on the reaction kinematics, expecially for Sub-GeV neutrinos, that have to be faithfully reproduced. In FLUKA , ν interactions are embedded in the PEANUT (see next section) nuclear environment[2], thus profiting from a longstanding development and benchmarking.

FLUKA HADRONIC MODELS

Since detailed descriptions of the FLUKA hadronic models and comparison with experimental data are available in the literature[4], we give here only a short summary. The high energy range (>5 GeV) is treated in the Glauber-Gribov formalism, that couples Glauber multiple scattering to a Dual Parton Model description of hadron-nucleon interactions. Nuclear effects on reaction products are described by a Generalized IntraNuclear Cascade (GINC) where the formation zone concept plays a fundamental role.

At lower energies, the intermediate energy hadronic model of FLUKA , called PEANUT is used. The reaction mechanism is modelled in PEANUT by explicit intranuclear cascade (INC) smoothly joined to statistical (exciton) preequilibrium emission [5]. INC modelling in PEANUT is highly sophisticated. Different nuclear densities are adopted for neutrons and protons, Fermi motion is defined locally including wave packet-like uncertainty smearing, the curvature of particle trajectories due to the nuclear potential is taken into account, binding energies are obtained from mass tables and updated after each particle emission, energy-momentum conservation including the recoil of the residual nucleus is ensured. Quantum effects are explicitely included: Pauli blocking, formation zone, nucleon antisymmetrization, nucleon-nucleon hard-core correlations, coherence length. Figure 1 shows the effects of the nuclear environments on the the kinematics of Quasi Elastic (QE) neutrino interactions. On a free nucleon, muons from the Charged Current reaction $\nu_\mu n \rightarrow \mu p$ reaction exhibit a clear momentum-angle correlation from the two body kinematics, while on Oxygen the distribution is smeared by Fermi momentum, and suppressed at low momentum transfer by the Pauli principle and by differences in binding energies (B.E.).

Formation zone, that can be naively assimilated to a "materialization" time, is essential in reducing the reinteraction probability, and has strong effects on the observed particle multiplicity and spectra, as shown in Fig.2 for the case of ν_μ interactions.

Pions deserve a special treatment, including many-body absorption based on in-medium characteristics of the Δ resonance, and motion in a resonant optical potential. The effect of pion absorption can be dramatic, for instance in a ν_μ interaction at 1 GeV on Ar, only 58% of the produced π escape from the target nucleus.

Independently from the original projectile energy, the equilibrium steps of the reaction include evaporation in competition with fission and gamma deexcitation. For light nuclei, a Fermi break-up model is implemented. Emission of energetic light fragments through the coalescence process is included all along the PEANUT reaction chain. The coalescence algorithm takes advantage of the knowledge of the space-time position of each emitted nucleon, as obtained from the cascade part or from the (geometry dependent) preequilibrium part. Particles are checked two-by-two, and they are lumped together whenever they are closer in phase-space than a given amount: the check is performed in the centre-of-mass system of the two particles, at the time which minimizes the relative spatial distance. Particles heavier than deuterons are formed by iterative accumulation of nucleons on clusters already formed in the previous steps of the process. Two examples are shown in Fig. 3.

Fragmentation and validation at CERF

The FLUKA evaporation model, which is based on the Weisskopf-Ewing approach, has been continuously updated along the years, with the inclusion, for instance, of sub-barrier emission, full level density formula, analytic solution of the emission widths. The latest upgrade is the extension to the evaporation of nuclear fragments

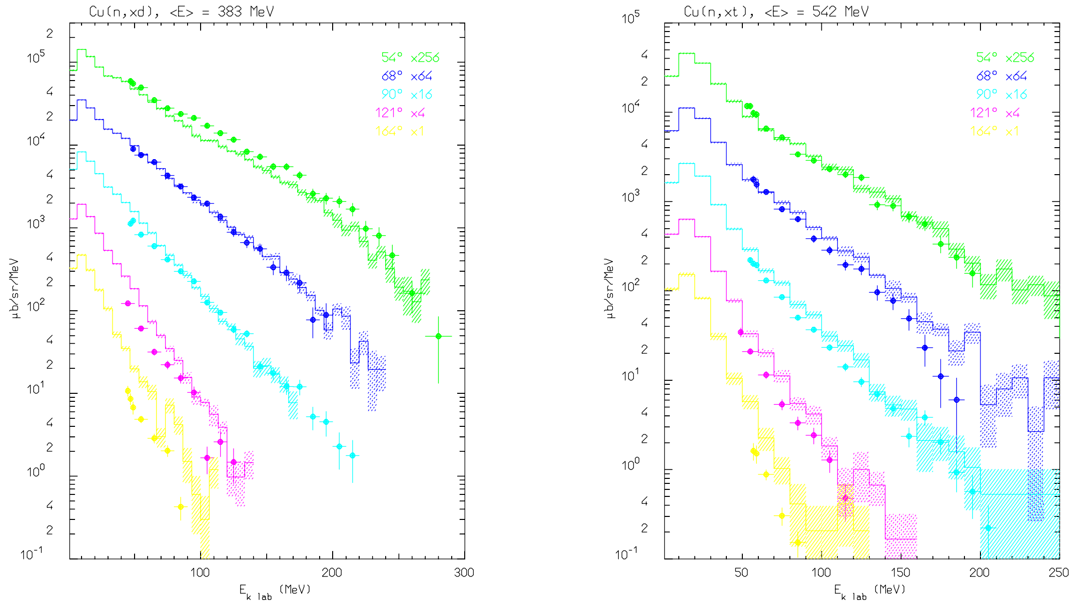

FIGURE 3. Deuteron (left) and triton (right) emission from 383 and 542 MeV neutrons on Cu. Data (symbols, from [3])

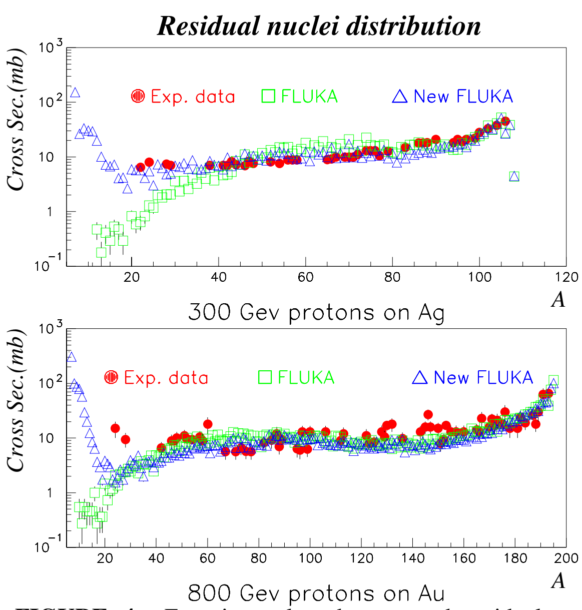

FIGURE 4. Experimental and computed residual nuclei mass distribution for Ag(p,x)X at 300 GeV (top) and Au(p,x)X at 800 GeV (bottom) (data from [6] for silver, and [7]for gold)

up to $A \leq 24$, with impressive improvements in the low mass region of residual nuclei distributions (see for instance Fig.4 and in the production of critical radioisotopes, like ^{7}Be. Radioisotope production and residual dose rate evaluation have been tested against experimental data [8] from a dedicated test beam at the CERF facility at CERN. Several material samples have been placed on the surface of a thick Cu target hit by a 120 GeV mixed p, π^+, K^+ beam. Thanks to showering in Cu, the samples were irradiated by broad band, mixed neutron and charged hadron spectra. An example of the results is shown in table 1, including the comparison between the standard FLUKA evaporation and the new evaporation-fragmentation model.

In-medium cross sections

The free NN scattering amplitudes and cross sections must be properly modified for medium effects (Pauli blocking, coherence effects, etc.). The resulting in medium cross sections are density-dependent and smaller than σ_{NNfree}. There are several approaches, see for instance [10, 11, 12], but one of open questions in microscopic models is the (proper) implementation of medium corrected nucleon cross sections. Double counting with explicit Pauli blocking (which is required to get physical events) is an issue, as well as proper correlations with the angular distribution. Figure 5 clearly shows the double counting when both in-medium cross sections and quantistic effects are taken into account (middle). The two alternative solutions, i.e. no in-medium σ with quantistic effects (left) and in-medium σ without quantistic effects (right) give similar results.

HEAVY IONS IN FLUKA

DPMJET [13], a Monte Carlo model for sampling hadron-hadron, hadron-nucleus and nucleus-nucleus collisions

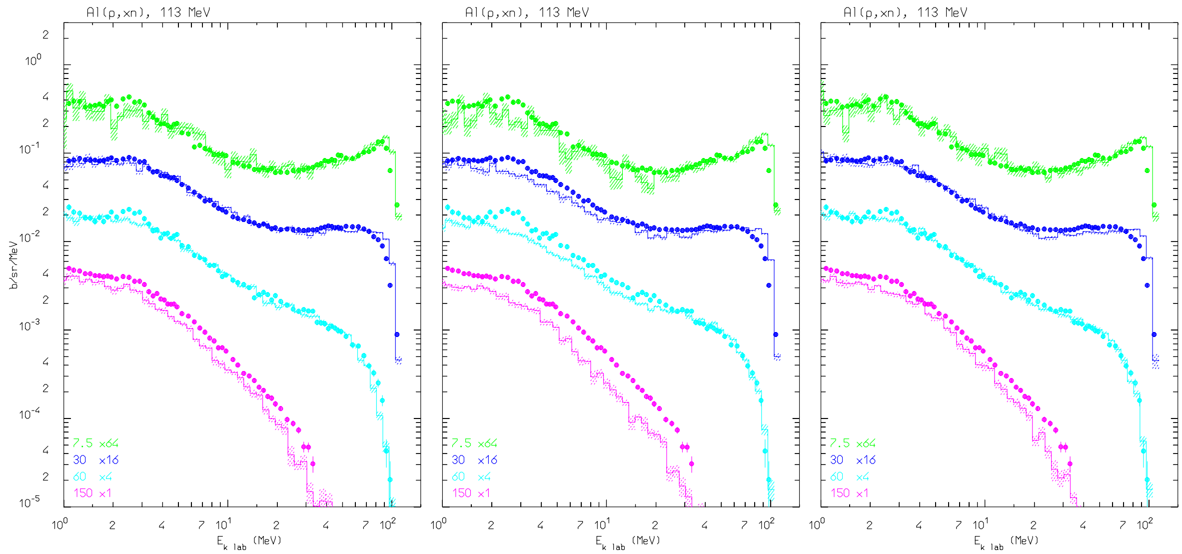

FIGURE 5. Double differential neutron distributions for Al(p,xn) at 113 MeV. "Normal" PEANUT (left), PEANUT with (Li) in-medium cross sections (center), PEANUT with in-medium cross sections and coherence length, correlation length, and nucleon hard core effects switched off (right). Histograms: computed with FLUKA ; symbols: experimental data from [9].

TABLE 1. Isotope production after the irradiation of a Stainless Steel sample at the CERF facility. Data are compared with the standard FLUKA evaporation model and with the new model including fragmentation

Isotope	Exp Bq/g %	STD FLUKA /Exp	NEW /Exp
Be 7	0.205 ± 24.3	0.096 ± 33	1.070 ± 30
Na 24	0.513 ± 4.3	0.278 ± 8.6	0.406 ± 13
K 43	1.08 ± 4.6	0.628 ± 8.7	0.814 ± 11
Ca 47	0.098 ± 25.1	0.424 ± 44	(0.295 ± 62)
Sc 44	13.8 ± 4.8	0.692 ± 5.8	0.622 ± 6.2
Sc 44m	6.51 ± 7.1	1.372 ± 8.1	1.233 ± 8.6
Sc 46	0.873 ± 8.3	0.841 ± 9.1	0.859 ± 9.5
Sc 47	6.57 ± 8.2	0.970 ± 9.7	1.050 ± 12
Sc 48	1.57 ± 5.2	1.266 ± 8.4	1.403 ± 11
V 48	8.97 ± 3.1	1.464 ± 3.8	1.354 ± 4.8
Cr 48	0.584 ± 6.7	1.084 ± 11	1.032 ± 12
Cr 51	15.1 ± 12.5	1.261 ± 12	1.231 ± 13
Mn 54	2.85 ± 10.1	1.061 ± 10	1.060 ± 11
Co 55	1.04 ± 4.6	1.112 ± 7.7	0.980 ± 10
Co 56	0.485 ± 7.6	1.422 ± 9.0	1.332 ± 10
Co 57	0.463 ± 10.7	1.180 ± 12	1.140 ± 12
Co 58	2.21 ± 5.9	0.930 ± 6.3	0.881 ± 6.9
Ni 57	3.52 ± 4.5	1.477 ± 6.5	1.412 ± 8.2

at accelerator and cosmic ray energies, was adapted and interfaced to the FLUKA program. The original interface to the DPMJET-II.53 version has recently been upgraded to comply with the DPMJET-III [14] version. DPMJET is based on the two component Dual Parton Model in connection with the Glauber formalism. FLUKA implements DPMJET as event generator to simulate nucleus-nucleus interactions exclusively. De-excitation and evaporation of the excited residual nuclei is performed by calling the FLUKA evaporation module. The RQMD-2.4 [15] is a relativistic QMD model which has been applied successfully to relativistic *AA* particle production over a wide energy range, from ≈ 0.1 GeV/n up to several hundreds of GeV/n. A RQMD-2.4 interface was developed to enable FLUKA to treat ion interactions from ≈ 100 MeV/n up to 5 GeV/n where DPMJET starts to be applicable. Several important modifications have been implemented in the RQMD code, in order to ensure energy-momentum conservation taking into account experimental binding energies, and to provide meaningful excitation energies for the residual fragments. The results of this modified model can be found in [16]

Electromagnetic Dissociation

Coulomb excitation of a target nucleus by the electromagnetic field of the projectile cannot be neglected in certain cases. It gets important at high energies and results in electromagnetic dissociation (ED) of the projectile nucleus. The lowest order diagram of the reaction, in which a high energy ion A_2 interacts inelastically with a target nucleus A_1 is depicted in Fig. (6). The cross section of this process σ_{EM} gets increasingly large with the target atomic number Z and energy of the incident ion owing to the rise in the photon flux density $n_{A_1}(\omega)$.

According to the concept of equivalent photons σ_{EM}

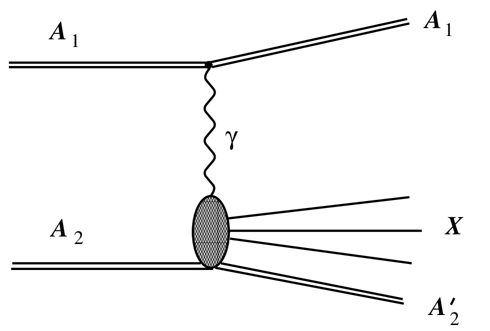

FIGURE 6. A one photon process induced by peripheral collision of two ions

factorizes into $n_{A_1}(\omega)$ and the cross section of the γA_2 interaction $\sigma_{\gamma A_2}(\omega)$:

$$\sigma_{EM} = \int \frac{\mathrm{d}\omega}{\omega} n_{A_1}(\omega)\sigma_{\gamma A_2}(\omega); \quad n_{A_1}(\omega) \propto Z_1^2 \quad (1)$$

where ω is the energy of the quasireal photon. The cross section of the ED process is already relevant for few GeV/n ions incident on heavy targets — $\sigma_{EM} \approx 1$ b, which should be compared with $\sigma_{nucl} \approx 5$ b for 1 GeV/n Fe on Pb.

The FLUKA model employs the standard approach developed for the evaluation of Eq. (1), which involves calculations of $n_{A_1}(\omega)$ in the Weizsäcker-Williams approximation, and the cross sections for the (quasireal) photon-nuclear reactions $\sigma_{\gamma A_2}(\omega)$. The latter are considered to be induced by the single (equivalent) photon absorption process.

In simulating ED the FLUKA model starts from elementary photon-nucleon and photo-nuclear cross sections stored in the program database. Most of data are taken from the experiments and are systematically updated. According to the FLUKA concept, all known physical processes responsible for electromagnetic excitation of nuclei — from the threshold of the photoneutron production reaction in the GDR region up to the TeV region are considered to contribute to $\sigma_{\gamma A_2}(\omega)$. Such an approach can render the simulation procedure very time consuming if one employs numerical integration which folds the considered equivalent photon spectrum $n_{A_1}(\omega)$ and the cross sections $\sigma_{\gamma A_2}(\omega)$. To avoid this problem, an analytical integration procedure has been developed for the latest version of the FLUKA model. In the energy intervals, in which theoretical or model description of $\sigma_{\gamma A_2}(\omega)$ can not be considered as acceptable, experimental data (e.g. the spectra in the GDR energy range) are approximated with Bezier curves. It should be emphasized that the developed algorithm allows fast automatic fit of the input data and thus fast upgrade of the cross section database for hundreds of nuclides. The fit is performed without losing accuracy of the measured photo-nuclear cross sections: systematic uncertainties introduced by the fit are substantially lower than typical discrepancies between data on photo-nuclear reactions from different groups.

Application of the developed algorithm in the simulation of fragmentation reactions of beam ions essentially improved an agreement with experimental data near the high-end spectrum (in the region of the highest Z). The simulated charge cross sections evaluated for 10.6 AGeV Au ions incident on Al and Pb targets are presented in Fig. (7) together with the data available in the range $53 \leq Z \leq 80$. We have also performed a simulation of the fragment charge cross sections for 158 AGeV Pb ions incident on six different targets for which experimental data were available in a much wider range of Z. The comparison of the simulated ED spectra with the data is shown with a dashed histogram in Fig. (8). This figure demonstrates how the role of the ED process gradually increases with Z of the target. A non-negligible contribution of the ED reaction is found in the case of nearly symmetric fragmentation of the projectile on heavy targets (Au and Pb) shown by the dashed histogram in the central region of the spectra.

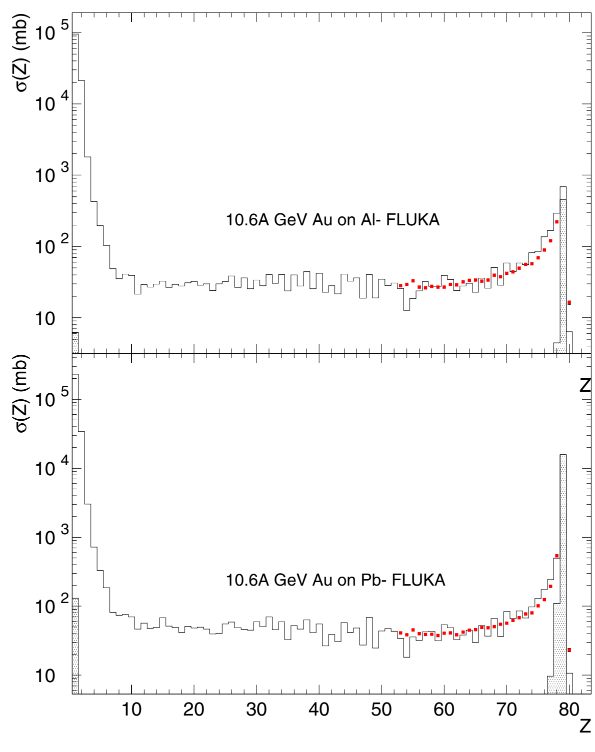

FIGURE 7. Fragment charge cross sections for 10.6 AGeV Au ions on Aluminum and Lead. Data (symbols) from [17], histograms are FLUKA (with DPMJET-III) predictions: the hatched histogram is the electromagnetic dissociation contribution

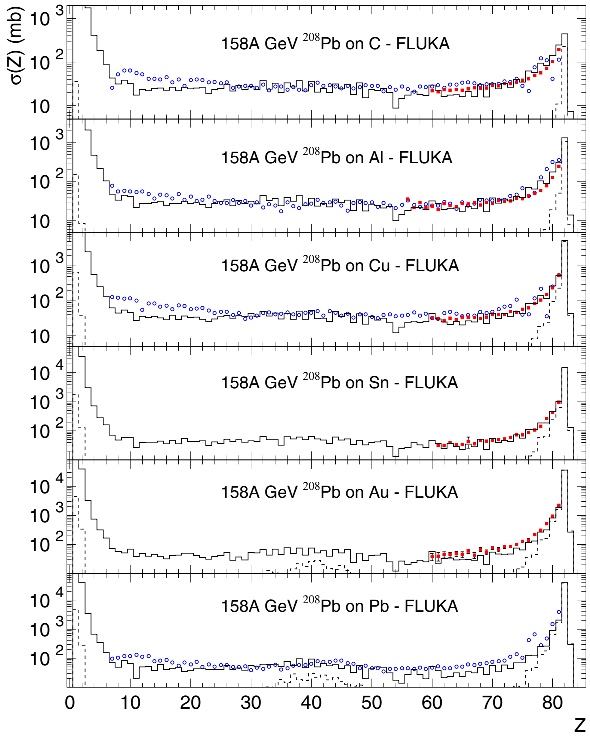

FIGURE 8. Fragment charge cross sections for 158 *A*GeV Pb ions on various targets. Data (symbols) from [18] (circles) and from [19] (squares), histograms are FLUKA (with DPMJET-III) predictions: the dashed histogram is the electromagnetic dissociation contribution

CONCLUSIONS

The FLUKA hadronic interaction models provide reliable and predictive results for a large variety of applications, from high energy physics to dosimetry and exotic applications. Nevertheless, further developments are foreseen, and further checking will be performed as soon as new experimental data will become available. In particular:

- Further improvement of the evaporation/fragmentation model, with extended benchmarking against activation data collected in real life accelerator environment.
- Further improvement of particle production simulation at few GeV, with refinement of the resonance production and reinteraction model and of the transition from "normal" to Glauber cascade.
- Rich development program for ions, including a new QMD model in place of the modified RQMDfor intermediate energies and a Boltzmann Master Equation model[20] covering the low energy range.

ACKNOWLEDGMENTS

This work was partially supported under: NASA Grant NAG8-1901, DOE contract DE-AC02-76SF00515, EU contract FI6R-CT-2003-508842.

REFERENCES

1. Fassò, A., Ferrari, A., Ranft, J., and Sala, P. R., "FLUKA: Status and Prospective for Hadronic Applications," in *Proocedings of the MonteCarlo 2000 Conference*, Springer-Verlag, Berlin, 2001, pp. 955–960.
2. Battistoni, G., Ferrari, A., Rubbia, A., and Sala, P. R., "The FLUKA nuclear cascade model applied to neutrino interactions," in *Proceedings of the NUINT02 workshop*, 2002, in press.
3. Franz, J., Koncz, P., Rossle, E., et al., *Nucl. Phys.*, **A510**, 774–802 (1990).
4. Ferrari, A., and Sala, P. R., "The Physics of High Energy Reactions," in *Proceedings of Workshop on Nuclear Reaction Data and Nuclear Reactors Physics, Design and Safety*, World Scientific, 1998, vol. 2, pp. 424–532.
5. Gadioli, E., and Hodgson, P. E., *Pre-equilibrium Nuclear Reactions*, Clarendon Press, Oxford, 1992.
6. Porile, N. T., Cole, G. D., and Rudy, C. R., *Phys. Rev.*, **C19**, 2288–2304 (1979).
7. Sihver, L., Aleklett, K., Loveland, W., McGaughey, P., et al., *Nucl. Phys.*, **A543**, 703–721 (1992).
8. Brugger, M., Khater, H., Mayer, S., et al., "Benchmark studies of induced radioactivity produced in LHC materials, Part I: Specific activities," in *proceedings of the ICRS10 conference*, 2004, in press.
9. Meier, M. M., Clark, D. A., Goulding, C. A., McClelland, J. B., Morgan, G. L., and Moss, C. E., *Nucl. Sci. and Eng.*, **102**, 310 (1989).
10. Li, G.-Q., Machleidt, R., and Zhuo, Y. Z., *Phys. Rev.*, **C48**, 1062 (1993).
11. Xiang-Zhou, C., FengJun, Wen-Qing, S., et al., *Phys. Rev.*, **C58**, 572–575 (1998).
12. Tripathi, R. K., Wilson, J. W., and Cucinotta, F. A., *Nucl. Instrum. Meth.*, **B152**, 425–431 (1999).
13. Ranft, J., *Phys. Rev.*, **D51**, 64–84 (1995).
14. Roesler, S., Engel, R., and Ranft, J., "The Monte Carlo event generator DPMJET-III," in *Proocedings of the MonteCarlo 2000 Conference*, Springer-Verlag, Berlin, 2001, pp. 1033–1038.
15. Sorge, H., Stöcker, H., and Greiner, W., *Nucl. Phys.*, **A498**, 567–576 (1989).
16. Andersen, V., Ballarini, F., Battistoni, G., et al., *Adv. Space Res.* (2004), in press.
17. Geer, L. Y., and Nilsen, J. K. B. S., *Phys. Rev.*, **C52**, 334–345 (1995).
18. Dekhissi, H., Giacomelli, G., Giorgini, M., et al., *Nucl. Phys.*, **A662**, 207–216 (2002).
19. Scheidenberger, C., et al., *Phys. Rev.*, **C70**, 014902 (2004).
20. Cerutti, F., Clivio, A., Gadioli, E., et al., "New results in comprehensive calculations of heavy ion interactions," in *Proceedings of this conference*, 2004.